Aquatic Sciences (2021) 83:30
https://doi.org/10.1007/s00027-021-00784-w

Aquatic Sciences

RESEARCH ARTICLE

Variability in fluorescent dissolved organic matter concentrations across diel to seasonal time scales is driven by water temperature and meteorology in a eutrophic reservoir

Dexter W. Howard[1] · Alexandria G. Hounshell[1] · Mary E. Lofton[1] · Whitney M. Woelmer[1] · Paul C. Hanson[2] · Cayelan C. Carey[1]

Received: 15 September 2020 / Accepted: 30 January 2021

Abstract

Freshwater reservoirs play a significant role in the global carbon cycle by processing and storing large quantities of dissolved organic matter (DOM). Quantifying the magnitude of DOM fluctuations across multiple temporal scales can advance our understanding of how the controls on reservoir carbon cycling may vary. We monitored fluorescent DOM (fDOM) using an in situ epilimnetic sensor at a ten-minute resolution over one year in a eutrophic reservoir in southwestern Virginia, USA with low dissolved organic carbon concentrations (2–6 mg L^{-1}). We determined the dominant time scales of variability and key environmental predictors of fDOM concentrations using continuous wavelet transforms and autoregressive time series modeling. Throughout the year, fDOM concentrations varied considerably, with maximum concentrations in the autumn (30.0 quinine sulfate units) and minimum concentrations in the spring (4.7 quinine sulfate units). The monthly time scale was the dominant time scale of variability, but the daily time scale was significant during the summer. Based on the autoregressive time series analysis, precipitation, water temperature, and shortwave radiation were important environmental predictors of fDOM on daily time scales, while water temperature alone best predicted monthly variability. Our study is one of the first to reveal substantial variability in fDOM concentrations during a full year, emphasizing the need for long-term, high-frequency in situ DOM monitoring to capture changes occurring on multiple time scales. By quantifying the variability and environmental predictors of fDOM on different time scales, we are able to better understand how and why DOM concentrations change throughout the year.

Keywords Continuous wavelet transforms · Dissolved organic carbon · Fluorescent dissolved organic matter · High frequency sensors · Reservoir limnology · Time series modeling

Introduction

Dissolved organic matter (DOM) in lakes and reservoirs is a complex mixture of many different organic compounds, with bulk DOM concentrations often represented as dissolved organic carbon (DOC; Curtis and Adams 1995). Freshwater DOM plays an important role in the global carbon cycle (Cole et al. 2007; Tranvik et al. 2009), in addition to influencing lake and reservoir ecosystem functioning and water quality (Kaplan et al. 2006; Williamson et al. 2015). Lake and reservoir DOM, whether allochthonous or autochthonous in origin, can either be buried in the sediments, mineralized and released to the atmosphere as carbon dioxide (CO_2) or methane (CH_4), or transported downstream (Tranvik et al. 2009; Hanson et al. 2015; Mendonça et al. 2017). Understanding the magnitude of DOM variability on different time scales and the environmental predictors of potential DOM pathways is needed to constrain the role of lakes and reservoirs in the global carbon cycle (Cole et al. 2007), especially as DOM and DOC dynamics may be changing due to altered climate and land use (Tranvik et al. 2009).

Variability in DOM concentrations has important consequences for lake and reservoir carbon balance, ecosystem functioning, and ecosystem services, such as drinking water

✉ Dexter W. Howard
dwh1998@vt.edu

[1] Department of Biological Sciences, Virginia Tech, Blacksburg, VA, USA

[2] Center for Limnology, University of Wisconsin, Madison, WI, USA

Published online: 22 February 2021

(Kaplan et al. 2006; Hanson et al. 2015; Williamson et al. 2015). DOM concentrations can influence light attenuation (Seekell et al. 2015), rates of microbial metabolism (Amon and Benner 1996; Minor and Stephens 2008; Williams et al. 2010), water chemistry (Schindler et al. 1992), plankton migration and food web structure (Leech and Williamson 2001; Miner and Kerr 2011; Williamson et al. 2015), and can lead to lake browning (Nicolle et al. 2012; Kritzberg et al. 2014). At high levels, DOM can decrease light availability and inhibit primary production, while at lower levels, DOM can stimulate primary production by releasing bound nutrients through photolysis (Seekell et al. 2015). In drinking water sources specifically, DOM can also serve as a precursor to disinfection by-product (DBP) formation (Kaplan et al. 2006; Tomlinson et al. 2016), which can be costly to treat. DBPs are formed in the water treatment process when DOM reacts with a disinfectant, such as chlorine, to form potentially carcinogenic compounds (Tomlinson et al. 2016).

Lakes and reservoirs exhibit a wide range of DOC concentrations worldwide (0.1 to > 300 mg L^{-1}), though most waterbodies exhibit concentrations between 1 to 20 mg L^{-1} (Sobek et al. 2007). Lake and reservoir DOM studies, however, have primarily focused on the summer stratified period, so the extent of DOM variability throughout the year, especially in the winter, remains understudied (but see Gonsior et al. 2013 and Denfeld et al. 2016). Variability in DOM concentrations can be due to many factors, including precipitation and associated runoff (Sadro and Melack 2012), photodegradation (Osburn et al. 2011; Cory and Kling 2018), microbial processing (Fasching et al. 2014), changes in water temperature (Gudasz et al. 2010; Dinsmore et al. 2013) or dissolved oxygen (DO; Bastviken et al. 2004), and phytoplankton excretion and uptake (Tittel and Kamjunke 2004; Zhang et al. 2009; Romera-Castillo et al. 2010), with the relative importance of different drivers varying with time scale. On diel scales, photodegradation can influence DOM concentrations in lakes and reservoirs by mineralizing DOC (Miller 1998; Osburn et al. 2011), especially in the well-lit epilimnion (Müller et al. 2014; Watras et al. 2016a). For example, Watras et al. (2016a) found that fluorescent DOM (fDOM) concentrations peak at night and decrease during the day in multiple lakes, suggesting that within-lake DOM processing and/or photodegradation can drive fDOM variability on the diel scale. In addition, microbial processing/uptake and phytoplankton excretion, as well as convective mixing entraining DOM from the metalimnion, have been shown to be important processes driving diel DOM variability (Watras et al. 2015).

On seasonal time scales, DOM variability is often driven by changing environmental conditions over the course of a year. Seasonal changes in precipitation can increase allochthonous carbon inputs via stream and overland flow and alter water residence time (WRT; Zwart et al. 2017). Decreases in WRT are associated with increases in DOC mineralization rates (Catalán et al. 2016), suggesting higher DOM lability in short WRT systems. In addition, increased temperature and DO, which vary seasonally due to stratification and mixing, have been shown to increase DOC mineralization rates (Bastviken et al. 2004; Lønborg et al. 2009; Gudasz et al. 2010). As mineralization rates increase due to increased temperature or higher DO concentrations, DOM concentrations decrease through its conversion to CO_2 and/or CH_4 (Bastviken et al. 2004; Cole et al. 2007). Water temperature has also been found to be positively associated with DOC on seasonal scales in streams due to biological production from allochthonous sources (Dinsmore et al. 2013). In addition, increases in air temperature can lead to increased export of soil DOC due to higher enzyme activity under warmer conditions, which increased DOC concentrations in streams and lakes in the United Kingdom (Freeman et al. 2001). Taken together, these seasonal changes in mineralization and inputs interact to drive changes in DOM concentrations in lakes and reservoirs.

As DOM concentrations can be highly variable across multiple time scales, obtaining high-frequency observations of DOM in lakes and reservoirs is important for improving our understanding of DOM drivers and dynamics. In situ fDOM sensors can be used to examine DOM variability on a range of time scales, from minutes to years, as fDOM represents a substantial fraction of the total DOC and DOM pools (Downing et al. 2009, 2012; Watras et al. 2011). fDOM sensors use ultraviolet (UV) light to detect the fluorescent component of DOM (Zhang et al. 2009; Downing et al. 2009), which is typically associated with terrestrial, humic-like organic matter, as determined by the Peak C region of excitation emission matrices (Coble et al. 2014; Fellman et al. 2010). Numerous studies have found fDOM to be a robust proxy for DOM as well as DOC in a range of freshwater ecosystems (e.g., Saraceno et al. 2009; Downing et al. 2009; Watras et al. 2011; Lee et al. 2015; Koenig et al. 2017).

Using high-frequency in situ fDOM sensors, continuous wavelet transforms, and time series modeling, we investigated the dominant time scales of variability of fDOM concentrations and their environmental predictors in the epilimnion of a dimictic reservoir over a full year, including in winter. In this study, we were interested in a broad range of time dynamics of DOM, which can be measured continuously at the minute scale with fDOM sensors while DOC observations, from traditional manual sampling, are usually only measured at weekly or longer periods. Our study addressed the following questions: (1) What are the dominant time scales of variability of fDOM across a year? and (2) What are the key environmental predictors of fDOM dynamics on daily to seasonal time scales?

Materials and methods

Study site

We examined fDOM dynamics in Falling Creek Reservoir (FCR), a small reservoir located in Vinton, Virginia, USA (37.30° N, 79.84° W; Fig. 1). FCR is classified as eutrophic and has a trophic state index (TSI) of 51 (Carlson and Simpson 1996; Supplementary Table 1). FCR is a drinking-water source located in a predominately deciduous forested catchment and is owned and operated by the Western Virginia Water Authority (see Gerling et al. 2016 for catchment land use and land cover data). FCR has a surface area of 0.12 km^2, a mean depth of 4 m, and a maximum depth of 9.3 m (Gerling et al. 2014). Its catchment area is 3.43 km^2, resulting in a catchment to surface area ratio of 29:1. The reservoir is historically dimictic, with intermittent ice cover during January to March, and thermal stratification from April to October (Carey 2019; Carey et al. 2019a). During the 2019 summer stratified period, FCR had a mean thermocline depth of 3 m, a mean light attenuation coefficient of 1.04 m^{-1}, and a mean photic zone depth of 5 m. The main inflow to FCR is via a forested stream that has a gauged weir (Fig. 1).

Field sampling

We deployed an EXO sonde, which measured fDOM, DO, temperature, and chlorophyll-*a* (YSI Incorporated, Yellow Springs, OH, USA) on ten-minute intervals at 1.6 m depth at the deepest site of FCR (Carey et al. 2020a; Fig. 1). We selected 1.6 m so the sensor was adjacent to a frequently-used outtake valve for water treatment. The EXO sonde was equipped with an automated wiper that operated on a ten-minute interval and was manually cleaned approximately weekly. We analyzed fDOM sonde data over a full calendar year, from 2 October 2018 through 1 October 2019. The fDOM sensor was calibrated prior to deployment following manufacturer instructions using distilled water and a one-point calibration to establish baseline concentrations and temperature corrections (Xylem 2019). The fDOM sensor measured excitation wavelengths at 365 ± 5 nm and emission wavelengths at 480 ± 40 nm, with a reported minimum detection limit of 0.07 quinine sulfate units (QSU). The wavelengths captured by the fDOM sensor are most closely related to the humic Peak C region as identified within an excitation-emission matrix (Xylem 2019; Coble et al. 2014). Humic peak C corresponds to fDOM that is characterized as humic-like, terrestrial, and allochthonous, and is often comprised of high molecular weight, highly aromatic and conjugated DOM molecules (Coble et al. 2014; Fellman et al. 2010).

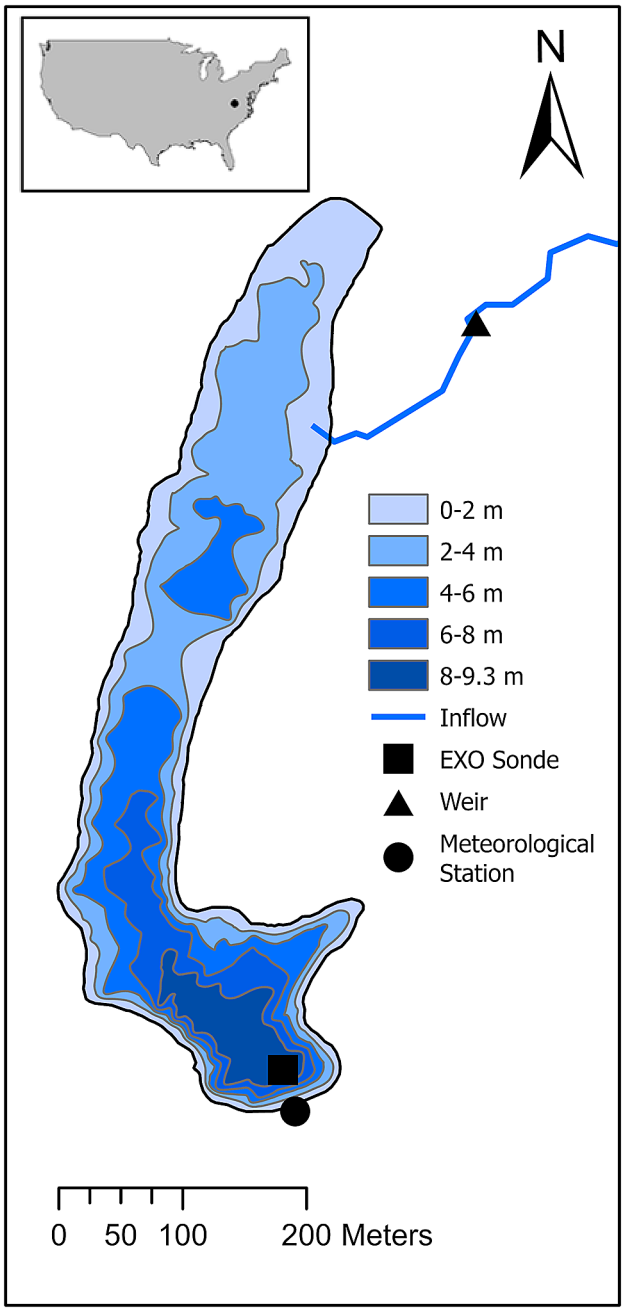

Fig. 1 Bathymetry map of Falling Creek Reservoir (FCR; 37.30° N, 79.84° W). Sampling sites (EXO Sonde, Weir, Meteorological Station) are denoted by the symbols on the map

As noted above, fDOM has often been used as a proxy for DOC in previous studies (e.g., Saraceno et al. 2009; Downing et al. 2009; Watras et al. 2011; Lee et al. 2015; Koenig et al. 2017). While our goal was not to predict DOC from fDOM, we compared the two variables to provide insights into reservoir DOM and DOC dynamics. Thus, we collected

intermittent in situ water samples for DOC analysis at the same site and depth (1.6 m) adjacent to the EXO sonde, as well as at 9 m at the same site and at the weir on the primary inflow stream (Carey et al. 2020b; Supplementary Figs. 1, 2). DOC sampling occurred twice weekly throughout the summer, weekly in the spring and fall, and monthly during the winter throughout the study period. Using a Van Dorn sampler (Wildco, Yulee, FL, USA) for the 1.6 m and 9 m samples and surface grabs for the inflow samples, we immediately filtered water through Whatman GF/F (0.7 µm) filters into acid-washed polypropylene bottles and stored frozen until analysis. Thawed DOC samples were poured into glass vials which had been acid-washed and combusted at 550 °C (USEPA 1979, 2009) and analyzed on an Elementar vario TOC cube (Elementar, Ronkonkoma, NY, USA) following US EPA Methods 415.1 and 415.3 (USEPA 1979, 2009), with a limit of quantitation of 0.41 mg L^{-1} and a minimum detection limit of 0.11 mg L^{-1}.

A research-grade meteorological station (Campbell Scientific, Logan, UT, USA) deployed at FCR's dam measured precipitation and incoming shortwave radiation every minute throughout the study period (Carey et al. 2020c; Fig. 1). Shortwave radiation was measured using a Hukseflux NR01 4-Component Net Radiometer with two SR01 pyranometers. The pyranometers capture a spectral range of 305–2800 nm (Carey et al. 2020c). The inflow weir on the primary tributary was equipped with an INW Aquistar PT2X pressure sensor (INW, Kirkland, WA) that was used to calculate stream inflow every fifteen minutes (Carey et al. 2020d; Fig. 1). WRT was calculated using the fifteen-minute inflow data averaged to daily values and assuming the volume of FCR was at full pond (3.1×10^5 m^3) following Gerling et al. (2014). FCR ice cover was monitored both visually and with water temperature sensors at the surface of the reservoir (Carey 2019; Supplementary Fig. 3 and Table 2); we defined spring mixis as the first date after the last ice-covered period with isothermal temperatures, following Bruesewitz et al. (2015).

Dominant time scales of variability

We used continuous wavelet transforms (CWTs) to determine dominant time scales of variability of fDOM in FCR, following the methods of Torrence and Compo (1998) and Carey et al. (2016). The CWTs applied scaled oscillating functions to the fDOM data to identify the relative importance of different time frequencies in the time series. The outputs of the CWTs are different power function values for each time scale on every sampling interval (Torrence and Compo 1998; Langman et al. 2010; Carey et al. 2016). Following the Nyquist theorem (Nyquist 1928; Shannon 1949), we determined the relative importance of time scales ranging from 20 min to 6 months for the year-long, ten-minute resolution fDOM data. CWT analysis was performed using R version 4.0.1 (R Core Team 2020) and package dplR (Bunn et al. 2020).

There were rare cases when fDOM values were missing, either due to sensor maintenance, malfunction, or extreme outliers. Outliers were defined as absolute values greater than two standard deviations (S.D. = 4.8 QSU) from previous and subsequent measurements. Outliers were removed, and all missing data were linearly interpolated prior to CWT analysis. In total, 0.6% of fDOM data points (n = 337 out of 52,544 total) were linearly interpolated. We used a Z-transform to normalize the time series data before CWT analysis, following Carey et al. (2016).

We used the Morlet continuous wavelet transforms (Torrence and Compo 1998) on the normalized time series. We analyzed 175 discrete time scales from 20 min (two times the minimum temporal frequency of measurement) to 6 months (half the total measurement period). To determine the dominant time scales of variability, we calculated the global power function by averaging the power function values for each time scale across the study period (Carey et al. 2016). To determine the significance of each scale, we compared the coefficients from our power function to coefficients from a red-noise spectrum, using a 95% significance level (Carey et al. 2016). We included a cone of influence (COI) to represent where edge effects may distort our results, especially for longer time scales (Torrence and Compo 1998; Carey et al. 2016).

Environmental predictors of fDOM variability

After the CWT analysis determined the daily and monthly time scales to be the most significant time scales of fDOM variability in FCR, we used autoregressive (AR) time series modeling to identify the most important environmental predictors of fDOM variability in FCR at these two time scales. We used AR models, rather than a cross-wavelet transform analysis, because we were interested in determining which combination of multiple environmental variables were most important for predicting fDOM on the daily and monthly scales. Additionally, cross-wavelets are primarily used to study the relationship between two time series (following Grinsted et al. 2004). AR modeling is commonly used to analyze ecological time series and is well-suited to our study because it accounts for temporal autocorrelation (Box and Pierce 1970; Hampton et al. 2013). AR time series analysis was performed using R version 4.0.1 (R Core Team 2020) with the stats (R Core Team 2020) and MuMIn packages (Barton 2020).

We created separate AR models for mean daily and mean monthly fDOM concentrations. To determine daily and monthly fDOM concentrations, we averaged the

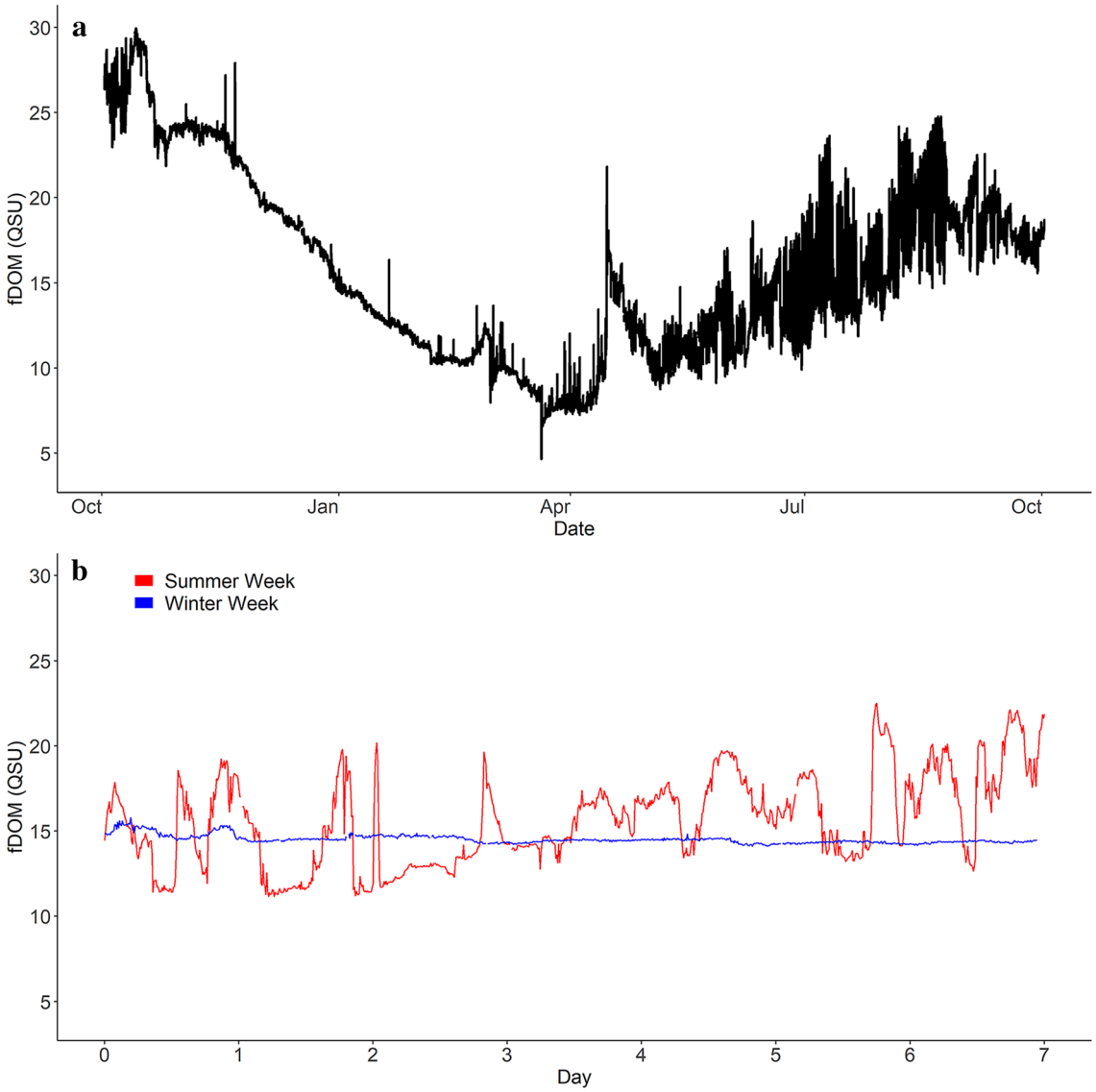

Fig. 2 **a** Time series of 10-min fDOM sensor observations from 2 October 2018–1 October 2019. **b** A representative summer week (1–7 July 2019; red) and a representative winter week (1–7 January 2019; blue) as a visual comparison of fDOM variability between seasons

ten-minute resolution fDOM data to each respective time scale. Next, we used a partial autocorrelation function (PACF) to determine significant lags and determined that only the first lag was needed to account for autocorrelation within the fDOM time series for both daily and monthly models (Supplementary Fig. 4).

We collated potential environmental predictor data on water temperature, DO percent saturation, chlorophyll-*a* concentration, WRT, inflow, shortwave radiation, and precipitation, and averaged all data to both daily and monthly scales. For the daily AR model, precipitation on a one day lag was included as a potential predictor in addition to same-day precipitation as it likely takes ~ 1 day for inflowing water to deliver terrestrial organic matter into the reservoir from the small, sloped, forested watershed. These environmental variables were selected based on literature suggesting they influence DOC and/or DOM concentrations (e.g., Bastviken et al. 2004; Gudasz et al. 2010; Osburn et al. 2011; Dinsmore et al. 2013; Tomlinson et al. 2016; Catalán et al. 2016). Spearman correlations were used to remove potential environmental predictors that were collinear with other predictors (Dormann et al. 2013). We excluded potential predictors with Spearman correlation rho values >|0.8| as aggregated over the daily and monthly time scales (Supplementary Tables 3 and 4). One-day lagged precipitation and precipitation from the same day were only weakly correlated (Spearman's $\rho = 0.3$), so both were included in the daily model (Supplementary

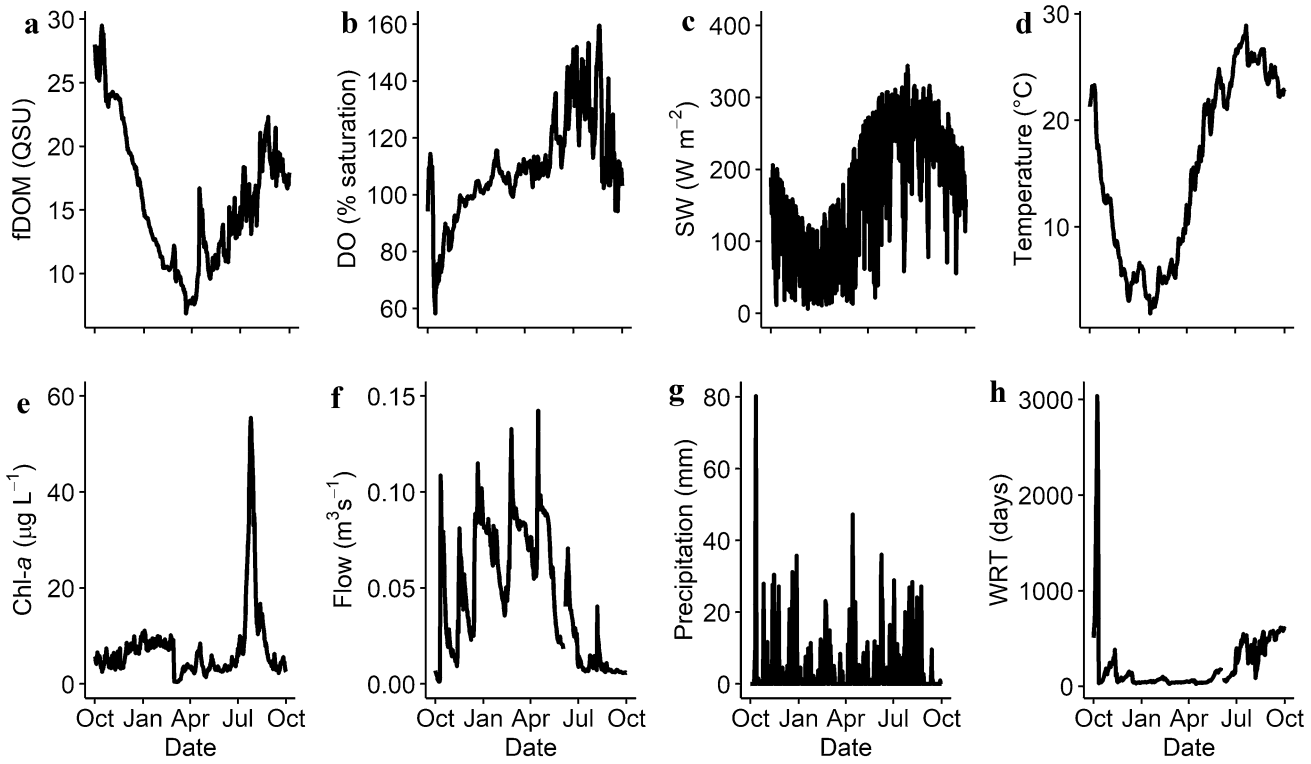

Fig. 3 Time series of daily aggregated fDOM and candidate environmental predictors of fDOM in Falling Creek Reservoir. **a** fDOM concentration, **b** dissolved oxygen (DO) percent saturation, **c** incoming shortwave radiation (SW), **d** water temperature, **e** chlorophyll-*a* (Chl-*a*), **f** inflow (flow), **g** precipitation, and **h** water residence time (WRT)

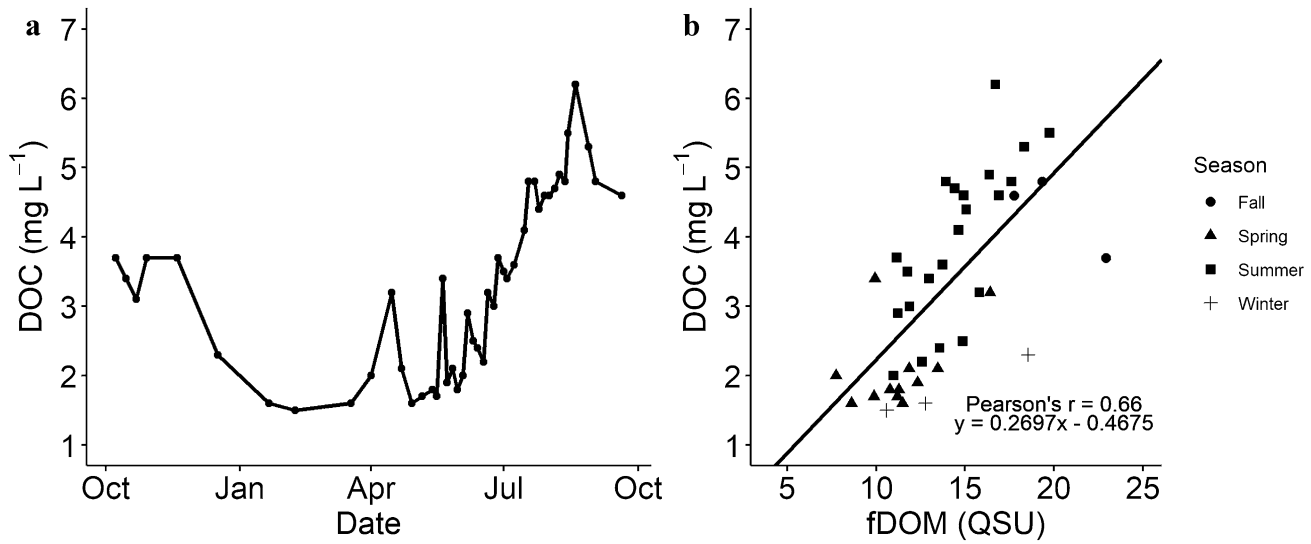

Fig. 4 **a** Timeseries of DOC concentrations from 7 October 2018–19 September 2019. **b** Correlation between DOC and fDOM (Pearson's r = 0.66). Observations within two weeks of fall turnover were removed from the statistical analysis (n = 4). Symbols designate different seasons throughout the year defined as: fall (circles), Winter (plus signs), Spring (triangles), and Summer (squares)

Table 3). We used a Z-transform on AR environmental predictor data to allow for comparison of the magnitude of coefficients in AR model results; fDOM data were not transformed for AR analysis.

Once we determined predictors and fDOM AR lag terms to include, we developed global models for both the daily and monthly time scales that included all possible combinations of potential non-collinear predictor variables. The predictors for the global daily fDOM model were the AR term, water temperature, DO percent saturation, chlorophyll-*a*, shortwave radiation, WRT, precipitation, and precipitation at a one day lag. The predictors for the global monthly fDOM model were the AR term, water temperature, DO percent saturation, chlorophyll-*a*, and monthly total (summed) precipitation. We then constructed AR models with all possible combinations of these predictor variables without interaction terms and a daily and monthly model using only the AR lag term. We used the corrected Akaike Information Criterion (AICc) to determine which models were the best predictors of fDOM concentrations for each time scale (Burnham and Anderson 2002). We report the top models for both daily and monthly fDOM (i.e., all models within two AICc units of the best-fitting model) and the model based solely on the AR lag term as a null model; the full model results are in Supplementary Tables 5 and 6.

Results

Observed variability in fDOM over time

fDOM concentrations exhibited substantial variability throughout the year (Fig. 2a), with maximum concentrations in October 2018 following passage of Hurricane Michael (30 QSU) and minimum concentrations in late March 2019 (4.7 QSU) (Figs. 2a, 3g). After fall turnover, which occurred on 21 October 2018, fDOM experienced a period of stable, yet elevated concentrations (~ 24 QSU) for approximately three weeks before declining throughout the winter (November 2018–March 2019). We note no changes in fDOM following spring mixis on 2 February 2019. The minimum fDOM concentration was observed in March 2019 at 4.7 QSU; fDOM increased again from April 2019 through September 2019.

In general, there was greater diel and hourly variability in fDOM concentrations in the summer (June–August) than in the winter (December–February; Fig. 2b). The mean daily (midnight to midnight) fDOM range in summer months was 5.61 ± 2.59 QSU, while the mean daily fDOM range in winter was 0.69 ± 0.66 QSU (Fig. 2b).

A comparison of fDOM and DOC during our study period indicates that fDOM and DOC were correlated (Pearson correlation $r = 0.66$; $p < 0.0001$; Fig. 4). Thus, while fDOM is capturing most of the DOC pool in FCR, there are likely other DOC compounds that are not being measured by the fDOM sensor. DOC concentrations measured at the weir on the primary inflow suggest similar DOC concentrations as the in-reservoir site at 1.6 m during the fall, winter, spring, and early summer (Supplementary Fig. 2). The increase in fDOM that occurred in the fall was associated with a similar increase in DOC concentrations at the same site while DOC concentrations at the inflow remained constant (Supplementary Figs. 1 and 2). Prior to fall turnover, the hypolimnion exhibited greater color and higher DOC concentrations than in the epilimnion, suggesting that the increase in fDOM at 1.6 m after turnover was likely due to an influx of organic matter from the hypolimnion (Supplementary Fig. 1).

Observed variability in potential environmental predictors of fDOM over time

Potential environmental predictors of fDOM showed varying trends throughout the year (Fig. 3). DO saturation, incoming shortwave radiation, and water temperature all exhibited expected seasonality (Fig. 3b–d). Water temperature at 1.6 m ranged from 2 to 30 °C over our sampling period, with maximum temperatures in late July and minimum temperatures in late January. In winter 2019, there were two short periods of ice cover that lasted from 21 to 23 January 2019 and 27 January to 1 February 2019 (Supplementary Table 2 and Fig. 3). Incoming shortwave radiation ranged from 6 to 344 W m^{-2} and followed similar temporal patterns as temperature. DO ranged from 58% to 160% saturation with peaks in August 2019 due to high primary production and minimum levels in October 2018 that coincided with fall turnover.

In contrast, inflow, precipitation (same day or lagged), WRT, and chlorophyll-*a* did not display obvious seasonal trends but did exhibit peaks which coincided with peaks in fDOM. Daily inflow ranged from 0.001 to 0.14 $m^3\ s^{-1}$ throughout our study period with peaks occurring throughout the year and low values occurring in September 2019. September 2019 was a particularly dry period with few precipitation events, which led to high WRT. Mean WRT was 215 days (median = 88, S.D. = 311, range = 25–3036) throughout the study period, with peaks in early October 2018 and September 2019. Precipitation increases in October 2018 due to Hurricane Michael coincided with rapid increases in fDOM. Chlorophyll-*a* concentrations ranged from 0 to 55 µg L^{-1}, with minimum concentrations in late March and maximum concentrations occurring during a phytoplankton bloom in July, with the chlorophyll-*a* peak coinciding with a peak in fDOM and increasing DOC concentrations.

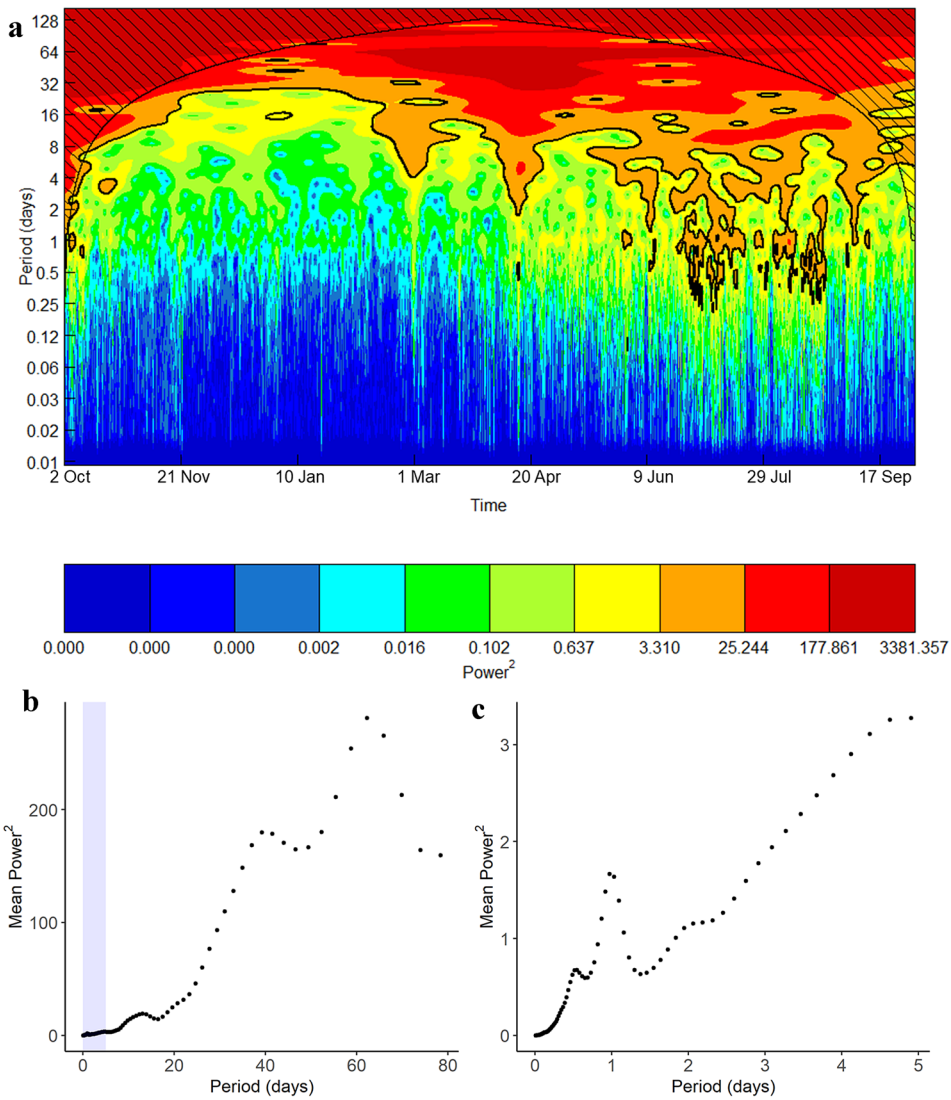

Fig. 5 **a** Continuous wavelet transform (CWT) showing the periodicity of fDOM concentrations through the full time series. The black contour represents 95% significance levels and the black hatching represents the cone of influence (COI) where edge effects may distort results. The color gradient represents power, in which darker red represents high power and darker blue represents low power. **b** The mean global power spectrum shows the dominant time scales aggregated over the entire monitoring period, based on the power value averaged across our study period time. The purple shaded region in **b** is plotted in **c**. **c** Mean global power over the range of 0–5 days. Note large differences in y-axis scale between **b** and **c**

Dominant time scales of fDOM variability

The CWT revealed that both monthly and daily scales were significant time scales of variability for fDOM, but their importance varied seasonally (Fig. 5). Overall, the monthly scale (~28–30 days) was the dominant time scale of variability during the year-long study (Fig. 5b). The monthly time scale had the highest global power value for time scales outside the COI; however, because our dataset was constrained to one year, edges of the monthly time scale results were located within the COI (Fig. 5a). Despite this, the majority of the monthly time scale was located outside of the COI and had a significantly larger global power value when compared to other time scales (Fig. 5b).

Despite the daily time scale having a lower global power value than the monthly time scale, it was still significant intermittently in July and August in 2019 (Fig. 5). This summer-time significance of daily time scales is visible in the global power spectrum analysis, in which the daily time scale had twice the global power than the preceding and following time scales (Fig. 5c). Throughout our year-long monitoring period, 62 days exhibited a significant daily time scale, with 50 (81%) of these days occurring in the summer. Of these 62 days, 69% (n = 43) occurred when water temperatures were greater than 25 °C, and 79% (n = 49) occurred when the daily mean incoming shortwave radiation was greater than 200 W m^{-2}, indicating that significant diel oscillations in fDOM were most likely to emerge on warm summer days with high mean irradiance.

Table 1 Equations and statistical values for daily and monthly AR models, ranked by best-fitting model for each time scale, as determined by AICc. The models listed are within two AICc units of each time scale's best-fitting model. We also included null models using only the AR lag term without environmental predictors. Environmental predictors are abbreviated as: chlorophyll-a (Chl-*a*), dissolved oxygen percent saturation (DO), water temperature (Temp), precipitation from same day or month (Precip), precipitation from previous day (Precip lag1), shortwave radiation (SW), and water residence time (WRT). The monthly models did not include SW or WRT and only included total summed monthly precipitation. The environmental predictor columns show the coefficient values for that predictor in the respective AR model; columns without coefficients listed were not included in a model

Model time scale	Chl-*a*	DO	Temp	Precip	Precip lag1	SW	WRT	Model equation	AICc	R^2	RMSE (QSU)
Daily 1			0.199	−0.079	0.226	−0.17		fDOM = 0.493 + 0.967(fDOM ARlag1) + 0.199(Temp) − 0.079 (Precip) + 0.226(Precip lag1) − 0.17(SW)	842.32	0.98	0.8
Daily 2		0.067	0.153	−0.079	0.23	−0.169		fDOM = 0.398 + 0.973(fDOM ARlag1) + 0.067(DO) + 0.153(Temp) − 0.079(Precip) + 0.23(Precip lag1) − 0.169(SW)	843.15	0.98	0.8
Daily 3			0.165		0.22	−0.123		fDOM = 0.449 + 0.97(fDOM ARlag1) + 0.165(Temp) + 0.22(Precip lag1) − 0.123(SW)	843.43	0.98	0.8
Daily 4	0.034		0.19	−0.081	0.224	−0.169		fDOM = 0.492 + 0.967(fDOM ARlag1) + 0.034(Chla) + 0.19(Temp) − 0.081(Precip) + 0.224(Precip lag1) − 0.169(SW)	843.74	0.98	0.8
Daily 5		0.067	0.119		0.224	−0.122		fDOM = 0.354 + 0.976(fDOM ARlag1) + 0.067(DO) + 0.119(Temp) + 0.224(Precip lag1) − 0.122(SW)	844.24	0.98	0.8
Daily lag only								fDOM = 0.273 + 0.981(fDOM ARlag1)	875.80	0.98	0.8

Model time scale	Chl-*a*	DO	Temp	Precip	Model equation	AICc	R^2	RMSE (QSU)
Monthly 1			2.784		fDOM = 2.858 + 0.839(fDOM ARlag1) + 2.783(Temp)	69.60	0.76	2.5
Monthly lag only					fDOM = 4.223 + 0.734(fDOM ARlag1)	72.85	0.53	3.5

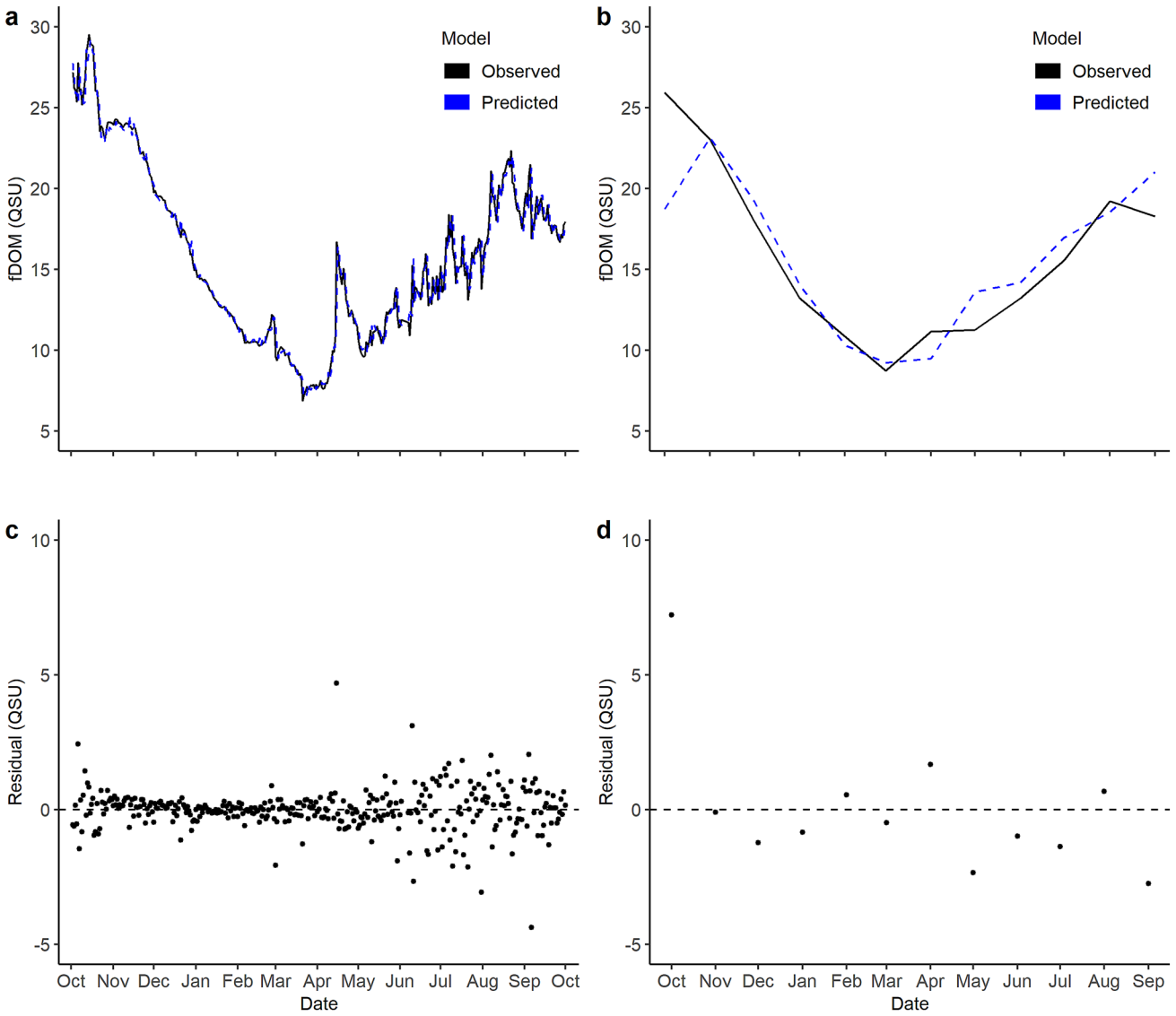

Fig. 6 Observed (black) and predicted (blue) fDOM concentrations for the **a** best-fitting AR daily model and **b** best-fitting AR monthly model. Model residuals are plotted for **c** daily fDOM and **d** monthly fDOM. Horizontal dashed lines indicate 0 for the residuals

Dominant predictors of fDOM on daily and monthly time scales

The AR models indicated that there were multiple environmental predictors of fDOM variability on the daily time scale (Table 1). The best-fitting model included an AR term, a positive relationship with precipitation from the previous day and water temperature and a negative relationship with incoming shortwave radiation and same day precipitation (RMSE = 0.8 QSU; Table 1). Four alternate models had AICc values within 2 units of the best-fitting model, indicating that their model fit was equally as good as the best-fitting model. Two of these alternate models included DO, while chlorophyll-*a* was included in one alternate model, all with a positive association with fDOM (Table 1). The AR lag term of fDOM was consistently an important driver in all of the daily models, but the models with environmental predictors were significantly better at predicting daily fDOM than the AR term alone, as indicated by a difference of > 30 AICc units between the best-fitting model and the AR term-only model (Table 1).

There was a strong level of agreement between observed and predicted fDOM concentrations in our best-fitting daily fDOM model (RMSE = 0.8 QSU; Table 1; Fig. 6a). The mean residual (observed minus predicted fDOM) was -0.002 ± 0.49 QSU from November to April but was higher from May through September (mean residual = -0.015 ± 1.00 QSU; Fig. 6b). The fDOM peaks during

October 2018 were not as well captured by the best-fitting daily model, with a mean October residual of 0.09 ± 0.80 QSU. The mean residual during the entire study period was extremely small ($20.6 \times 10^{-15} \pm 0.76$ QSU), indicating that the best-fitting daily model was a good predictor of daily fDOM.

Water temperature was the dominant driver of fDOM variability on monthly scales (Table 1). The best-fitting monthly model was driven by a positive relationship with water temperature (RMSE = 2.50 QSU). The best-fitting monthly model predicted monthly fDOM reasonably well throughout the year (RMSE = 2.5 QSU; mean residual = $-4.88 \times 10^{-15} \pm 2.59$ QSU), but did not capture fDOM variability during the fall (September 2019, October 2018; Fig. 6d). The best-fitting monthly model over-predicted fDOM in September 2019 (residual = − 2.75 QSU) and under-predicted the fDOM peak in October 2018 (residual = 7.22 QSU). The best-fitting monthly model also over-predicted monthly fDOM in May 2019 (residual = − 2.34 QSU). Similar to the daily models, the AR term was found to be an important driver in the monthly models, but the models with environmental predictors had lower AICc than the AR term-only model (monthly AICc difference of ~ 3 units; Table 1).

The best-fitting monthly and daily models differed in their ability to accurately predict fDOM concentrations. The best-fitting monthly model explained less variability in the observed fDOM data than the daily models, likely due to the aggregation of data to the monthly scale, but still explained monthly fDOM reasonably well with an R^2 of 0.76 and an RMSE of 2.50 QSU (Table 1). While AICc cannot be compared between daily and monthly models, the best-fitting daily fDOM model had substantially lower RMSE (0.80 QSU) and higher R^2 (0.98) than the best-fitting monthly model.

Discussion

We found that the monthly time scale was the dominant time scale of variability for fDOM throughout our year-long study and was largely predicted by water temperature. The daily time scale was also significant during the summer and predicted by precipitation from the previous day and same-day precipitation, water temperature, and shortwave radiation. Quantifying fDOM variability and identifying the key environmental predictors on different time scales improves our understanding of how and why DOM concentrations may be changing throughout the year. Our finding of minimal daily fDOM variability in winter months, even when there is no ice cover, is valuable in expanding our understanding of year-round DOM dynamics. Below, we discuss the implications of our findings for reservoir DOM variability and carbon cycling.

DOM cycling in reservoirs

This study represents one of the first to assess fDOM dynamics in a reservoir, as the majority of long-term (i.e., at least 3 months) fDOM studies to date have been conducted in naturally-formed lakes (Ryder et al. 2012; Watras et al. 2015, 2016b; National Ecological Observatory Network 2020). While naturally-formed lakes and reservoirs share many similar characteristics, there are several key differences that allow for interesting comparisons between the two waterbody types. First, reservoirs on average have seven times higher catchment to surface area ratios in the U.S., which can lead to higher runoff and DOM loading rates (Doubek and Carey 2017). Second, reservoirs tend to have half the WRT of natural lakes in the U.S., which influences DOM mineralization rates (Hayes et al. 2017; Doubek et al. 2019). This is particularly important as shorter WRT can lead to increased inputs of highly-labile DOM (Zwart et al. 2017; Duffy et al. 2018). Third, reservoir construction has long-term effects on ecosystem biogeochemical pathways, through transformation of river and floodplain ecosystems to reservoirs, which inherently differ from natural lakes (e.g., Maeck et al. 2013; Gerling et al. 2016). Due to construction of dams on former rivers or wetlands, organic matter can build up in reservoir sediments (Downing et al. 2008; Maeck et al. 2013; Deemer et al. 2016). Over time, accumulated sediment organic matter can increase the release of labile organic carbon into the water column, resulting in higher and more variable fDOM and DOC concentrations in reservoirs as compared to naturally formed lakes (Clow et al. 2015). Thus, high-frequency monitoring of fDOM dynamics may be particularly important for human-made reservoirs, which have been shown to be highly variable freshwater ecosystems (Górniak et al. 2002).

Despite the waterbody type differences described above, FCR exhibits a similar range and concentration of fDOM and DOC over time as compared to naturally formed lakes. In FCR, we observed fDOM concentrations ranging from 4.7 to 30.0 QSU over a full year (Fig. 2a), with correlated DOC concentrations ranging from 1.5 to 6.2 mg L^{-1} (mean: 3.3 mg L^{-1}; Fig. 4). In a literature search of waterbodies with sub-daily fDOM measurements over several months, we found seven lakes or reservoirs with comparable fDOM data sets to FCR. Milford Reservoir and Lakes Feeagh, Crampton, and Suggs all exhibit higher concentrations and ranges of fDOM than FCR, while Lakes Barco and Mendota exhibited smaller ranges and lower fDOM concentrations (Table 2). Little Rock Lake was the only system with similar fDOM range and concentration to FCR (Table 2). Additionally, we compared FCR to lakes in Wisconsin, USA (Lead PI

Table 2 Mean and range of epilimnetic DOC and fDOM for lakes worldwide, calculated from the multiple days to years of available data for each waterbody aggregated together

Waterbody name	Naturally-formed lake or reservoir	Location	Mean DOC (mg L^{-1})	DOC range (mg L^{-1})	Mean fDOM (QSU)	fDOM range (QSU)	Sampling period	Sampling interval	Description (derived from reference)	References
Falling Creek (this study)	Reservoir	Virginia, USA	3.3	1.5–6.2	15.7	4.7–30.0	October 2018–October 2019	fDOM: 10 min DOC: weekly–monthly	Small eutrophic reservoir	Carey et al. (2020a, b)
Barco	Lake	Florida, USA	0.7		6.5	0.9–10.5	17 January–4 November 2019; DOC: 1986–1987	fDOM: 5 min DOC: seasonally	Clear soft water lake	National Ecological Observatory Network (2020); James (1991)
Crampton	Lake	Wisconsin, USA	4.0		23.8	12.5–61.7	fDOM: 29 July–5 November 2019 DOC: July–August 2000	fDOM: 5 min	Clear oligotrophic	National Ecological Observatory Network (2020); Hanson et al. (2003)
Feeagh	Lake	Mayo, Ireland		7.7–12.3		36.4–77.5	fDOM: March 2010–December 2011 DOC: July 2010–June 2011	fDOM: 2 min DOC: not specified	Oligotrophic, humic lake	Ryder et al. (2012)
Little Rock	Lake	Wisconsin, USA	3.2		14.5	8.4–30	fDOM: 26 June–6 October 2019 DOC: not specified	fDOM: 5 min	Seepage lake	National Ecological Observatory Network (2020); Watras et al. (2016b)
Mendota	Lake	Wisconsin, USA	5.6	2.7–15.5	9.8	5.8–12.8	fDOM: April–November 2019 DOC: 1996–2018	fDOM: daily average DOC: monthly–seasonally	Eutrophic lake	Lead PI (2020a; b)
Milford	Reservoir	Kansas, USA			51.0	32.4–60.6	May–September 2016	15 min intervals on 25–26 May, 8–10 June, 20–21 July, 14–15 September	Eutrophic reservoir	King (2019)
Suggs	Lake	Florida, USA	22.6		222.2	119.9–279.2	fDOM: 7 January–14 December 2019 DOC: 1986–1987	fDOM: 5 min DOC: seasonally	Dark water lake	National Ecological Observatory Network (2020); James (1991)

Columns with missing data did not have sources reporting those values. Sampling occurred at the dam or deepest site of each lake or reservoir

2020a) and Sweden (Environmental data MVM 2020) that had comparable DOC data. FCR had lower mean DOC concentrations than lakes in both Wisconsin and Sweden but had a larger range over multiple months than many Swedish lakes (Supplementary Table 7). By comparing results from FCR to waterbodies around the world, we highlight the need to consider a broad gradient of ecosystems, including lakes and reservoirs across latitudes, to develop a more global understanding of fDOM in these ecosystems.

Drivers of fDOM on daily and monthly time scales

The monthly time scale was the dominant time scale of fDOM variability and primarily driven by water temperature. We initially expected temperature would be negatively correlated with fDOM, as increasing water temperature is linked to increasing DOM mineralization at lake sediments (Gudasz et al. 2010), but observed a positive relationship, likely due to an increase in biological activity and primary production during warmer months (Freeman et al. 2001; Weyhenmeyer and Karlsson 2009; Dinsmore et al. 2013). In FCR, the positive correlation between temperature and fDOM could be due to increased primary production, which can increase autochthonous DOM concentrations as a result of phytoplankton excretion and degradation (Zhang et al. 2009; Romera-Castillo et al. 2010). This mechanism is supported by observed increases in fDOM and DOC shortly after the chlorophyll-*a* maximum in late July (Figs. 3a, e, 4a). Alternatively, higher terrestrial primary production in warm summer conditions can increase freshwater allochthonous DOC concentrations (Pagano et al. 2014). Other waterbodies have exhibited a similar pattern to FCR, e.g., a study of 1041 Swedish lakes found that DOC exhibited a positive relationship with air temperature across the region (Weyhenmeyer and Karlsson 2009).

Following our expectations, shortwave radiation was negatively correlated with daily fDOM concentrations. Increased solar radiation can lead to increased photodegradation and a resulting decrease in DOM concentrations in surface waters (Osburn et al. 2011; Ward and Cory 2020). Other studies using fDOM sensors have also found that shortwave radiation decreased fDOM concentrations on daily to seasonal time scales in lake epilimnia (Müller et al. 2014; Watras et al. 2016a). Müller et al. (2014) found that solar radiation led to a 25–50% reduction in CDOM over the course of four months while daily chromophoric DOM (CDOM) had a coefficient of variation (CV) up to 15% due to solar radiation. In FCR, we observed a greater level of variability during the day (CV = 34%; Fig. 2b), but did not observe a decrease in concentrations throughout the summer as predicted by Müller et al. (2014), likely because FCR has relatively high allochthonous and autochthonous DOM loads because of its short WRT and eutrophic state, respectively.

Precipitation from the previous day was found to be an important positive driver of daily fDOM concentrations while precipitation on the same day was a negative driver (Table 1). Previous studies have shown both positive relationships between precipitation and aquatic DOC (Sadro and Melack 2012; Dinsmore et al. 2013; Zwart et al. 2017), and negative relationships between precipitation and DOC due to dilution (Engstrom 1987). The mechanisms likely driving these patterns are immediate dilution or flushing due to precipitation, thereby decreasing DOC concentrations on the day of precipitation, followed by greater delivery of organic matter into the reservoir that increase reservoir DOC on subsequent days. We also note that Hurricane Michael led to rapid increases in fDOM (up to 30 QSU) in early October 2018, suggesting that episodic storm events may also be important to fDOM dynamics in reservoir ecosystems (Fig. 3g). However, this may not be true for all systems; for example, an extreme storm event with > 50 mm of precipitation in a 2-h period at Lough Feeagh, Ireland had no noticeable effect on DOC in this humic lake (de Eyto et al. 2016). Altogether, our results suggest that hydrology and the magnitude of precipitation interact to control the relationship between precipitation and reservoir fDOM in Falling Creek Reservoir.

Implications for winter limnology

Our analysis of a year-long, high-frequency fDOM dataset allowed us to examine fDOM dynamics through the winter. Despite major projected changes in the duration of winter processes, especially ice cover (Hampton et al. 2017), few studies have explored winter fDOM dynamics (Downing et al. 2009; Ryder et al. 2012; Koenig et al. 2017). FCR has historically experienced ice cover lasting over a month in the winter, but during our study, the reservoir only had two short periods of ice cover lasting 3–6 days (Carey 2019, Supplementary Table 2 and Fig. 3). Although FCR experienced intermittent ice cover, there were no notable differences in patterns of fDOM concentrations through time during ice covered vs. non-ice covered periods (Supplementary Table 8). This suggests ice cover had little influence on fDOM concentrations during the winter of 2019, but we note that the ice cover in FCR was intermittent and thin during the study period. We note that the daily scale did not emerge as significant during the winter months, likely due to reduced variability in daily temperature, solar radiation, and primary production during the winter as compared to the summer. As ice cover becomes more dynamic in many waterbodies (Sharma et al. 2019), determining the effects of intermittent ice cover and a longer open-water period on fDOM should be a priority for future studies.

Limitations and possible next steps

While our study is useful in informing DOM patterns and drivers over a year, we acknowledge some limitations. Additional years of data would allow us to determine if the dominant time scale of variability changes across longer time scales; however, we note that our study is one of the first to successfully capture fDOM dynamics during the winter, including during brief ice covered conditions. Additional data would also allow us to better understand the effect of fall turnover on fDOM concentrations. Fall turnover had major effects on fDOM concentrations in October 2018, disrupting the seasonal pattern for nearly three weeks, when concentrations stabilized at ~ 24 QSU before gradually decreasing throughout the winter (Fig. 2a). Finally, including additional environmental variables known to be strongly correlated to fDOM variability, such as photodegradation rates and microbial activity (Bastviken et al. 2003; Williams et al. 2010; Osburn et al. 2011; Müller et al. 2014), would likely help constrain fDOM variability on multiple time scales.

In addition, the specific wavelengths captured by the fDOM EXO sonde have important implications for our understanding of fDOM variability and environmental drivers in this ecosystem. Specifically, the fDOM captured in this study was constrained to the terrestrial, humic-like, Peak C region of excitation emission fluorescence (Coble et al. 2014; Fellman et al. 2010), indicating that we are likely missing a large portion of fDOM (Miller et al. 2009). This has important implications for a eutrophic ecosystem like FCR, where a significant contribution to the DOC and fDOM pools may be from autochthonous sources (Supplementary Fig. 2). Additional studies would be needed to discriminate the relative contributions of the two sources to fDOM variability in reservoirs.

Conclusions

By identifying the dominant time scales of fDOM variability and key environmental predictors, our work contributes to an improved understanding of reservoir DOM and carbon cycling. As reservoirs process and store significant amounts of carbon, our work highlights the variability of reservoir DOM dynamics throughout the year and demonstrates the similarities and differences between reservoir and lake ecosystems. In eutrophic reservoirs with short WRT like FCR, constant allochthonous and autochthonous inputs of DOM may increase diel DOM variability and processing rates relative to glacially-formed lakes. For example, Watras et al. (2016a) observed oscillations up to 0.28 mg L^{-1} in fDOM-correlated DOC concentrations over 24 h in the epilimnia of glacially-formed lakes in northern Wisconsin. In comparison, daily summer fDOM in FCR ranged up to 5.6 QSU, which corresponds to 1.0 ± 0.7 mg L^{-1} DOC as calculated using the observed fDOM-DOC correlation (Fig. 4; Watras et al. 2016a).

Additionally, our study provides a baseline for comparing summer versus winter fDOM concentrations and variability. We highlight the importance of fDOM variability on daily and monthly timescales throughout the year, which were largely attributed to seasonal and diurnal patterns of temperature variability. As changes in temperature become more prevalent in the future due to global change, we expect to see greater increases in DOM concentrations in lakes and reservoirs. This has significant implications for not only our understanding of DOM cycling in FCR, but more broadly organic carbon cycling in lakes and reservoirs experiencing global change.

Electronic supplementary material The online version of this article (https://doi.org/10.1007/s00027-021-00784-w) contains supplementary material, which is available to authorized users.

Acknowledgements We thank the Western Virginia Water Authority for their long-term support and access to field sites. Bethany Bookout provided critical sensor maintenance and Ryan McClure helped with fieldwork and modeling. Barbara Niederlehner and Heather Wander helped analyze DOC samples. The Virginia Tech Reservoir group and FCR carbon team provided the collaborative foundation for this study. We would also like to thank two anonymous Reviewers and Associate Editor Dr. Yu-Ping Chin for their constructive feedback, which substantially improved the manuscript. We gratefully acknowledge our funding sources, including the National Science Foundation (NSF) grants DEB-1753639, DEB-1753657, CNS-1737424, DEB-1926050, DBI-1933016, and DBI-1933102, a Schoenholtz Fellowship from the Virginia Water Resources Research Center, the Virginia Tech Global Change Center, and Fralin Life Science Institute at Virginia Tech.

Author contributions DWH, MEL, and CCC conceived the research project. DWH led data curation, data analyses, and writing with significant help and support from AGH, MEL, and CCC. AGH and MEL guided the project's progress with DWH. AGH provided critical biogeochemical expertise and CCC developed wavelet transform analysis. MEL and WMW provided help with analytical chemistry analysis and WMW helped with sensor data QA/QC and time series modeling. PCH provided expertise on modeling and organic matter cycling. All coauthors provided feedback on writing and approved the final version of this manuscript.

Funding This study was financially supported by the National Science Foundation (NSF) grants DEB-1753639, DEB-1753657, CNS-1737424, DEB-1926050, DBI-1933102, and DBI-1933016, a Schoenholtz Fellowship from the Virginia Water Resources Research Center, the Virginia Tech Global Change Center, and Fralin Life Science Institute at Virginia Tech.

Availability of data and material All data used in this analysis are published in the Environmental Data Initiative repository: Ice cover data (Carey 2019; https://doi.org/10.6073/pasta/eecfa7ba08f9ee233ece6df0e9cbcb3a). Inflow data (Carey et al. 2020d; https://doi.org/10.6073/pasta/30caad87e3e5aafd1f9ace836c94d2fa). Temperature CTD profiles (Carey et al. 2019a; https://doi.org/10.6073/pasta/1fc7d2a5c69c6a651793dba06d375ae2). DOC and phosphorus

concentrations (Carey et al. 2020b; https://doi.org/10.6073/pasta/0d29704769868facec3e238e64d35557) EXO sonde (Carey et al. 2020a; https://doi.org/10.6073/pasta/b888ac006ef4ca601f63e2703d7476b9). Meteorological data (Carey et al. 2020c; https://doi.org/10.6073/pasta/ea47ae493c7025d61245287649895e60). Secchi data (Carey et al. 2019b; https://doi.org/10.6073/pasta/e9b8ee83bc7fad6dcdf439a41ad80a3c). Filtered chlorophyll-*a* data (Carey et al. 2020e; https://doi.org/10.6073/pasta/4103be6062b768867e1f3b016665a35c).

Code availability Code used for CWT and AR analyses can be found at https://doi.org/10.5281/zenodo.4430029 (Howard 2021).

Compliance with ethical standards

Conflict of interest The authors declare no competing interests.

References

Amon RMW, Benner R (1996) Photochemical and microbial consumption of dissolved organic carbon and dissolved oxygen in the Amazon River system. Geochim Cosmochim Acta 60:1783–1792. https://doi.org/10.1016/0016-7037(96)00055-5

Barton K (2020) MuMIn: Multi-Model Inference. R package version 1.43.17. https://CRAN.R-project.org/package=MuMIn

Bastviken D, Olsson M, Tranvik L (2003) Simultaneous measurements of organic carbon mineralization and bacterial production in oxic and anoxic lake sediments. Microb Ecol 46:73–82. https://doi.org/10.1007/s00248-002-1061-9

Bastviken D, Persson L, Odham G, Tranvik L (2004) Degradation of dissolved organic matter in oxic and anoxic lake water. Limnol Oceanogr 49:109–116. https://doi.org/10.4319/lo.2004.49.1.0109

Box GEP, Pierce DA (1970) Distribution of residual autocorrelations in autoregressive-integrated moving average time series. J Am Stat Assoc 65:1509–1526

Bruesewitz DA, Carey CC, Richardson DC, Weathers KC (2015) Under-ice thermal stratification dynamics of a large, deep lake revealed by high-frequency data. Limnol Oceanogr 60:347–359. https://doi.org/10.1002/lno.10014

Bunn A, Korpela M, Biondi F, Campelo F, Mérian P, Qeadan F, Zang C (2020) dplR: Dendrochronology Program Library in R. R package version 1.7.1. https://CRAN.R-project.org/package=dplR

Burnham KP, Anderson DR (2002) Model selection and multimodel inference: a practical information-theoretic approach, second. Springer, New York

Carey CC (2019) Ice cover data for Falling Creek Reservoir, Vinton, Virginia, USA for 2013-2019 ver 1. Environ Data Initiat. https://doi.org/10.6073/pasta/eecfa7ba08f9ee233ece6df0e9cbcb3a. Accessed 9 Apr 2020

Carey CC, Hanson PC, Lathrop RC, St. Amand AL (2016) Using wavelet analyses to examine variability in phytoplankton seasonal succession and annual periodicity. J Plankton Res 38:27–40. https://doi.org/10.1093/plankt/fbv116

Carey CC, Lewis AS, McClure RP, Gerling AB, Doubek JP, Chen S, Lofton ME, Hamre KD (2019a) Time series of high-frequency profiles of depth, temperature, dissolved oxygen, conductivity, specific conductivity, chlorophyll a, turbidity, pH, oxidation-reduction potential, photosynthetic active radiation, and descent rate for Beaverdam Reservoir, Carvins Cove Reservoir, Falling Creek Reservoir, Gatewood Reservoir, and Spring Hollow Reservoir in Southwestern Virginia, USA 2013-2019 ver 10. Environ Data Initiat. https://doi.org/10.6073/pasta/1fc7d2a5c69c6a651793dba06d375ae2. Accessed 3 May 2020

Carey CC, Gerling AB, Doubek JP, Hamre KD, McClure RP, Lofton ME, Farrell KJ, Wander HL (2019b) Secchi depth data and discrete depth profiles of photosynthetically active radiation, temperature, dissolved oxygen, and pH for Beaverdam Reservoir, Carvins Cove Reservoir, Falling Creek Reservoir, Gatewood Reservoir, and Spring Hollow Reservoir in southwestern Virginia, USA 2013-2018 ver 7. Environ Data Initiat. https://doi.org/10.6073/pasta/e9b8ee83bc7fad6dcdf439a41ad80a3c. Accessed 3 Dec 2020

Carey CC, Bookout BJ, Woelmer WM, Lewis AS (2020a) Time series of high-frequency sensor data measuring water temperature, dissolved oxygen, conductivity, specific conductivity, total dissolved solids, chlorophyll a, phycocyanin, and fluorescent dissolved organic matter at discrete depths in Falling Creek Reservoir, Virginia, USA in 2018-2019 ver 4. Environ Data Initiat. https://doi.org/10.6073/pasta/b888ac006ef4ca601f63e2703d7476b9. Accessed 13 Mar 2020

Carey CC, Wander HL, Woelmer WM, Lofton ME, Gerling AB, McClure RP, Doubek JP, Niederlehner BR, Farrell KJ (2020b) Water chemistry time series for Beaverdam Reservoir, Carvins Cove Reservoir, Falling Creek Reservoir, Gatewood Reservoir, and Spring Hollow Reservoir in southwestern Virginia, USA 2013-2019 ver 7. Environ Data Initiat. https://doi.org/10.6073/pasta/0d29704769868facec3e238e64d35557. Accessed 3 Dec 2020

Carey CC, Bookout BJ, Lofton ME, McClure RP (2020c) Time series of high-frequency meteorological data at Falling Creek Reservoir, Virginia, USA 2015-2019 ver 4. Environ Data Initiat. https://doi.org/10.6073/pasta/ea47ae493c7025d61245287649895e60. Accessed 13 Mar 2020

Carey CC, Hounshell AG, Lofton ME, Bookout BJ, Corrigan RS, Gerling AB, McClure RP, Woelmer WM (2020d) Discharge time series for the primary inflow tributary entering Falling Creek Reservoir, Vinton, Virginia, USA 2013-2020 ver 6. Environ Data Initiat. https://doi.org/10.6073/pasta/30caad87e3e5aafd1f9ace836c94d2fa. Accessed 13 Mar 2020

Carey CC, Lofton ME, Woelmer WM, Wynne JH, Doubek JP, Hamre KD, and Niederlehner BR (2020e) Filtered chlorophyll a time series for Beaverdam Reservoir, Carvins Cove Reservoir, Claytor Lake, Falling Creek Reservoir, Gatewood Reservoir, Smith Mountain Lake, and Spring Hollow Reservoir in southwestern Virginia, USA during 2014-2019 ver 1. Environ Data Initiat. https://doi.org/10.6073/pasta/4103be6062b768867e1f3b016665a35c. Accessed 3 Dec 2020

Carlson RE, Simpson J (1996) A coordinator's guide to volunteer lake monitoring methods. North Am Lake Manag Soc

Catalán N, Marcé R, Kothawala DN, Tranvik LJ (2016) Organic carbon decomposition rates controlled by water retention time across inland waters. Nat Geosci 9:501–504. https://doi.org/10.1038/ngeo2720

Clow DW, Stackpoole SM, Verdin KL, Butman DE, Zhu Z, Krabbenhoft DP, Striegl RG (2015) Organic carbon burial in lakes and reservoirs of the conterminous United States. Environ Sci Technol 49:7614–7622. https://doi.org/10.1021/acs.est.5b00373

Coble PG, Spencer RGM, Baker A, Reynolds DM (2014) Aquatic organic matter fluorescence. In: Aquatic organic matter fluorescence, pp 75–122

Cole JJ, Prairie YT, Caraco NF et al (2007) Plumbing the global carbon cycle: integrating inland waters into the terrestrial carbon budget. Ecosystems 10:172–185. https://doi.org/10.1007/s10021-006-9013-8

Cory RM, Kling GW (2018) Interactions between sunlight and microorganisms influence dissolved organic matter degradation

along the aquatic continuum. Limnol Oceanogr Lett 3:102–116. https://doi.org/10.1002/lol2.10060
Curtis PJ, Adams HE (1995) Dissolved organic matter quantity and quality from freshwater and saltwater lakes in east-central Alberta. Biogeochemistry 30:59–76. https://doi.org/10.1007/BF02181040
de Eyto E, Jennings E, Ryder E, Sparber K, Dillane M, Dalton C, Poole R (2016) Response of a humic lake ecosystem to an extreme precipitation event: physical, chemical, and biological implications. Inl Waters 6:483–498. https://doi.org/10.1080/iw-6.4.875
Deemer BR, Harrison JA, Li S et al (2016) Greenhouse gas emissions from reservoir water surfaces: a new global synthesis. Bioscience 66:949–964. https://doi.org/10.1093/biosci/biw117
Denfeld BA, Kortelainen P, Rantakari M, Sobek S, Weyhenmeyer GA (2016) Regional variability and drivers of below Ice CO2 in boreal and subarctic lakes. Ecosystems 19:461–476. https://doi.org/10.1007/s10021-015-9944-z
Dinsmore KJ, Billett MF, Dyson KE (2013) Temperature and precipitation drive temporal variability in aquatic carbon and GHG concentrations and fluxes in a peatland catchment. Glob Chang Biol 19:2133–2148. https://doi.org/10.1111/gcb.12209
Dormann CF, Elith J, Bacher S et al (2013) Collinearity: A review of methods to deal with it and a simulation study evaluating their performance. Ecography (Cop) 36:27–46. https://doi.org/10.1111/j.1600-0587.2012.07348.x
Doubek JP, Carey CC (2017) Catchment, morphometric, and water quality characteristics differ between reservoirs and naturally formed lakes on a latitudinal gradient in the conterminous United States. Inl Waters 7:171–180. https://doi.org/10.1080/20442041.2017.1293317
Doubek JP, Carey CC, Lavender M, Winegardner K, Beaulleu M, Kelly PT, Pollard AI, Straile D (2019) Calanoid copepod zooplankton density is positively associated with water residence time across the continental United States. PLoS ONE 14:1–22. https://doi.org/10.1371/journal.pone.0209567
Downing JA, Cole JJ, Middelburg JJ, Striegl RG, Duarte DM, Kortelainen P, Prairie YT, Laube KA (2008) Sediment organic carbon burial in agriculturally eutrophic impoundments over the last century. Global Biogeochem Cycles 22:GB1018. https://doi.org/10.1029/2006GB002854
Downing BD, Boss E, Bergamaschi BA, Fleck JA, Lionberger MA, Ganju NK, Schoellhamer DH, Fujii R (2009) Quantifying fluxes and characterizing compositional changes of dissolved organic matter in aquatic systems in situ using combined acoustic and optical measurements. Limnol Oceanogr Methods 7:119–131. https://doi.org/10.4319/lom.2009.7.119
Downing BD, Pellerin BA, Bergamaschi BA, Saraceno JF, Kraus TEC (2012) Seeing the light: the effects of particles, dissolved materials, and temperature on in situ measurements of DOM fluorescence in rivers and streams. Limnol Oceanogr Methods 10:767–775. https://doi.org/10.4319/lom.2012.10.767
Duffy CJ, Dugan HA, Hanson PC (2018) The age of water and carbon in lake-catchments: a simple dynamical model. Limnol Oceanogr Lett 3:236–245. https://doi.org/10.1002/lol2.10070
Engstrom BR (1987) Influence of vegetation and hydrology on the humus budgets of Labrador lakes. Can J Fish Aquat Sci 44:1306–1314
Environmental data MVM (2020) Swedish University of Agricultural Sciences (SLU). Data host lakes and watercourses, and Data host agricultural land. http://miljodata.slu.se/mvm/2020-05-26
Fasching C, Behounek B, Singer GA, Battin TJ (2014) Microbial degradation of terrigenous dissolved organic matter and potential consequences for carbon cycling in brown-water streams. Sci Rep 4:4981. https://doi.org/10.1038/srep04981
Fellman JB, Hood E, Spencer RGM (2010) Fluorescence spectroscopy opens new windows into dissolved organic matter dynamics in freshwater ecosystems: a review. Limnol Oceanogr 55:2452–2462. https://doi.org/10.4319/lo.2010.55.6.2452
Freeman C, Evans CD, Monteith DT, Reynolds B, Fenner N (2001) Export of organic carbon from peat soils. Nature 412:785. https://doi.org/10.1038/35090628
Gerling AB, Browne RG, Gantzer PA, Mobley MH, Little JC, Carey CC (2014) First report of the successful operation of a side stream supersaturation hypolimnetic oxygenation system in a eutrophic, shallow reservoir. Water Res 67:129–143. https://doi.org/10.1016/j.watres.2014.09.002
Gerling AB, Munger ZW, Doubek JP, Hamre KD, Gantzer PA, Little JC, Carey CC (2016) Whole-catchment manipulations of internal and external loading reveal the sensitivity of a century-old reservoir to hypoxia. Ecosystems 19:555–571. https://doi.org/10.1007/s10021-015-9951-0
Gonsior M, Schmitt-Kopplin P, Bastviken D (2013) Depth-dependent molecular composition and photo-reactivity of dissolved organic matter in a boreal lake under winter and summer conditions. Biogeosciences 10:6945–6956. https://doi.org/10.5194/bg-10-6945-2013
Górniak A, Zieli P, Jekatierynczuk-Rudczyk E, Grabowska M, Suchowolec T (2002) The role of dissolved organic carbon in a shallow lowland reservoir ecosystem—a long-term study. Acta Hydrochim Hydrobiol 30:179–189
Grinsted A, Moore JC, Jevrejeva S (2004) Application of the cross wavelet transform and wavelet coherence to geophysical time series. Nonlinear Process Geophys Eur Geosci Union 11:561–566
Gudasz C, Bastviken D, Steger K, Premke K, Sobek S, Tranvik LJ (2010) Temperature-controlled organic carbon mineralization in lake sediments. Nature 466:478–481. https://doi.org/10.1038/nature09186
Hampton SE, Homes EE, Scheef LP et al (2013) Quantifying effects of abiotic and biotic drivers on community dynamics with multivariate autoregressive (MAR) models. Ecology 94:2663–2669
Hampton SE, Galloway AWE, Powers SM et al (2017) Ecology under lake ice. Ecol Lett 20:98–111. https://doi.org/10.1111/ele.12699
Hanson PC, Bade DL, Carpenter SR, Kratz TK (2003) Lake metabolism: relationships with dissolved organic carbon and phosphorus. Limnol Oceanogr 48:1112–1119. https://doi.org/10.4319/lo.2003.48.3.1112
Hanson PC, Pace ML, Carpenter SR, Cole JJ, Stanely EH (2015) Integrating landscape carbon cycling: research needs for resolving organic carbon budgets of lakes. Ecosystems 18:363–375. https://doi.org/10.1007/s10021-014-9826-9
Hayes NM, Deemer BR, Corman JR, Razavi NR, Strock KE (2017) Key differences between lakes and reservoirs modify climate signals: a case for a new conceptual model. Limnol Oceanogr Lett 2:47–62. https://doi.org/10.1002/lol2.10036
Howard DW (2021) dwh77/Variability_FCR_fDOM_MS_Code: Second release of associated code (Version v2.0.0). Zenodo. https://doi.org/10.5281/zenodo.4430029
James RT (1991) Microbiology and chemistry of acid lakes in Florida: II. Seasonal relationships. Hydrobiologia 213:227–240. https://doi.org/10.1007/BF00016424
Kaplan LA, Newbold JD, Van Horn DJ, Dow CL, Aufdenkampe AK, Jackson JK (2006) Organic matter transport in New York City drinking-water-supply watersheds. J North Am Benthol Soc 25:912–927. https://doi.org/10.1899/0887-3593(2006)025[0912:omtiny]2.0.co;2
King LR (2019) Water-quality data from two sites on Milford Lake, Kansas, May 25–26, June 8–10, July 20–21, and September 14–15, 2016: U.S. Geological Survey data release. https://doi.org/10.5066/F78S4P4M

Koenig LE, Shattuck MD, Snyder LE, Potter JD, McDowell WH (2017) Deconstructing the effects of flow on DOC, nitrate, and major ion interactions using a high-frequency aquatic sensor network. Water Resour Res 53:655–673. https://doi.org/10.1002/2017WR020739

Kritzberg ES, Granéli W, Björk J, Brönmark C, Hallgren P, Nicolle A, Persson A, Hansson LA (2014) Warming and browning of lakes: Consequences for pelagic carbon metabolism and sediment delivery. Freshw Biol 59:325–336. https://doi.org/10.1111/fwb.12267

Langman OC, Hanson PC, Carpenter SR, Hu YH (2010) Control of dissolved oxygen in northern temperate lakes over scales ranging from minutes to days. Aquat Biol 9:193–202. https://doi.org/10.3354/ab00249

Lead PI N, Magnuson J, Carpenter S, Stanley E (2020a) North temperate lakes LTER: chemical limnology of primary study lakes: nutrients, pH and carbon 1981—current ver 52. Environ Data Initiat. https://doi.org/10.6073/pasta/8359d27bbd91028f222d923a7936077d. Accessed 10 Jun 2020

Lead PI N, Magnuson J, Carpenter S, Stanley E (2020b) North temperate lakes LTER: high frequency data: meteorological, dissolved oxygen, chlorophyll, Phycocyanin—Lake Mendota Buoy 2006—current ver 31. Environ Data Initiat. https://doi.org/10.6073/pasta/c03b39550e79d002d82a2281f8546c78. Accessed 10 Jun 2020

Lee EJ, Yoo GY, Jeong Y, Kim KU, Park JH, Oh NH (2015) Comparison of UV-VIS and FDOM sensors for in situ monitoring of stream DOC concentrations. Biogeosciences 12:3109–3118. https://doi.org/10.5194/bg-12-3109-2015

Leech DM, Williamson CE (2001) In situ exposure to ultraviolet radiation alters the depth distribution of Daphnia. Limnol Oceanogr 46:416–420. https://doi.org/10.4319/lo.2001.46.2.0416

Lønborg C, Davidson K, Álvarez-Salgado XA, Miller AEJ (2009) Bioavailability and bacterial degradation rates of dissolved organic matter in a temperate coastal area during an annual cycle. Mar Chem 113:219–226. https://doi.org/10.1016/j.marchem.2009.02.003

Maeck A, Delsontro T, Mcginnis DF, Fischer H, Flury S, Schmidt M, Fietzek P, Lorke A (2013) Sediment trapping by dams creates methane emission hot spots. Environ Sci Technol 47:8130–8137. https://doi.org/10.1021/es4003907

Mendonça R, Müller RA, Clow D, Verpoorter C, Raymond P, Tranvik LJ, Sobek S (2017) Organic carbon burial in global lakes and reservoirs. Nat Commun 8:1694. https://doi.org/10.1038/s41467-017-01789-6

Miller WL (1998) Effects of UV radiation on aquatic humus: photochemical principles and experimental considerations. In: Hessen DO, Tranvik LJ (eds) Aquatic humic substances. Ecological studies (analysis and synthesis), vol 133. Springer. Berlin, Heidelberg, pp 135–153

Miller MP, McKnight DM, Chapra SC, Williams MW (2009) A model of degradation and production of three pools of dissolved organic matter in an alpine lak. Limnol Oceanogr 54:2213–2227. https://doi.org/10.4319/lo.2009.54.6.2213

Miner BE, Kerr B (2011) Adaptation to local ultraviolet radiation conditions among neighbouring Daphnia populations. Proc R Soc B 278:1306–1313. https://doi.org/10.1098/rspb.2010.1663

Minor E, Stephens B (2008) Dissolved organic matter characteristics within the Lake Superior watershed. Org Geochem 39:1489–1501. https://doi.org/10.1016/j.orggeochem.2008.08.001

Müller RA, Kothawala DN, Podgrajsek E, Sahlée E, Koehler B, Tranvik LJ, Weyhenmeyer GA (2014) Hourly, daily, and seasonal variability in the absorption spectra of chromophoric dissolved organic matter in a eutrophic, humic lake. J Geophys Res Biogeosci 119:1985–1998. https://doi.org/10.1002/2014JG002719

National Ecological Observatory Network (2020) Data product DP1.20288.001, water quality. Provisional data downloaded from http://data.neonscience.org on May 27, 2020. Battelle, Boulder, CO, USA NEON

Nicolle A, Hallgren P, Von Einem J, Kritzberg ES, Granéli W, Persson A, Brönmark C, Hansson LA (2012) Predicted warming and browning affect timing and magnitude of plankton phenological events in lakes: a mesocosm study. Freshw Biol 57:684–695. https://doi.org/10.1111/j.1365-2427.2012.02733.x

Nyquist H (1928) Certain topics in telegraph transmission theory. Trans Am Inst Electr Eng 47:617–644. https://doi.org/10.1109/T-AIEE.1928.5055024

Osburn CL, Wigdahl CR, Fritz SC, Saros JE (2011) Dissolved organic matter composition and photoreactivity in prairie lakes of the U.S. Great Plains. Limnol Oceanogr 56:2371–2390. https://doi.org/10.4319/lo.2011.56.6.2371

Pagano T, Bida M, Kenny JE (2014) Trends in levels of allochthonous dissolved organic carbon in natural water: a review of potential mechanisms under a changing climate. Water 6:2862–2897. https://doi.org/10.3390/w6102862

R Core Team (2020) R: A language and environment for statistical computing. R Foundation for Statistical Computing, Vienna, Austria. https://www.R-project.org/

Romera-Castillo C, Sarmento H, Álvarez-Salgado XA, Gasol JM, Marrasé C (2010) Production of chromophoric dissolved organic matter by marine phytoplankton. Limnol Oceanogr 55:446–454. https://doi.org/10.4319/lo.2010.55.1.0446

Ryder E, Jennings E, de Eyto E, Dillane M, NicAonghusa C, Pierson D, Moore K, Rouen M, Poole R (2012) Temperature quenching of CDOM fluorescence sensors: Temporal and spatial variability in the temperature response and a recommended temperature correction equation. Limnol Oceanogr Methods 10:1004–1010. https://doi.org/10.4319/lom.2012.10.1004

Sadro S, Melack J (2012) The effect of an extreme rain event on the biogeochemistry and ecosystem metabolism of an oligotrophic high-elevation lake, Arctic. Antarct Alp Res 44:222–231. https://doi.org/10.1657/1938-4246-44.2.222

Saraceno JF, Pellerin BA, Downing BD, Boss E, Bachand PAM, Bergamaschi BA (2009) High-frequency in situ optical measurements during a storm event: assessing relationships between dissolved organic matter, sediment concentrations, and hydrologic processes. J Geophys Res 114:G00F09. https://doi.org/10.1029/2009JG000989

Schindler DW, Bayley SE, Curtis PJ, Parker BR, Stainton MP, Kelly CA (1992) Natural and man-caused factors affecting the abundance and cycling of dissolved organic substances in precambrian shield lakes. Hydrobiologia 229:1–21. https://doi.org/10.1007/BF00006987

Seekell DA, Lapierre JF, Karlsson J (2015) Trade-offs between light and nutrient availability across gradients of dissolved organic carbon concentration in Swedish lakes: Implications for patterns in primary production. Can J Fish Aquat Sci 72:1663–1671. https://doi.org/10.1139/cjfas-2015-0187

Shannon CE (1949) Communication in the presence of noise. Proc Inst Radio Eng 37:10–21. https://doi.org/10.1109/JRPROC.1949.232969

Sharma S, Blagrave K, Magnuson JJ, O'Reilly CM, Oliver S, Batt RD, Magee MR, Straile D, Weyhenmeyer GA, Winslow L, Woolway RI (2019) Widespread loss of lake ice around the Northern Hemisphere in a warming world. Nat Clim Chang 9:227–231. https://doi.org/10.1038/s41558-018-0393-5

Sobek S, Tranvik LJ, Prairie YT, Kortelainen P, Cole JJ (2007) Patterns and regulation of dissolved organic carbon: An analysis of 7,500 widely distributed lakes. Limnol Oceanogr 52:1208–1219. https://doi.org/10.4319/lo.2007.52.3.1208

Tittel J, Kamjunke N (2004) Metabolism of dissolved organic carbon by planktonic bacteria and mixotrophic algae in lake neutralisation

experiments. Freshw Biol 49:1062–1071. https://doi.org/10.1111/j.1365-2427.2004.01241.x

Tomlinson A, Drikas M, Brookes JD (2016) The role of phytoplankton as pre-cursors for disinfection by-product formation upon chlorination. Water Res 102:229–240. https://doi.org/10.1016/j.watres.2016.06.024

Torrence C, Compo GP (1998) A practical guide to wavelet analysis. Bull Am Meteorol Soc 79:61–78

Tranvik LJ, Downing JA, Cotner JB et al (2009) Lakes and reservoirs as regulators of carbon cycling and climate. Limnol Oceanogr 54:2298–2314. https://doi.org/10.4319/lo.2009.54.6_part_2.2298

USEPA (1979) Method 415.1.0, organic carbon, total by combustion or oxidation. EPA-600/4-79-020, Environmental Monitoring Systems Laboratory, ORD, USEPA, Cincinnati, Ohio 45268

USEPA (2009) Method 415.3, Revision 1.2, Determination of total organic carbon and specific UV absorbance at 254 nm in source water and drinking water. EPA-600/R-09/122, National Exposure Research Laboratory, Office of Research and Development, USEPA, Cincinnati, Ohio 45268

Ward CP, Cory RM (2020) Assessing the prevalence, products, and pathways of dissolved organic matter partial photo-oxidation in arctic surface waters. Environ Sci Process Impacts 22:1214–1223. https://doi.org/10.1039/c9em00504h

Watras CJ, Hanson PC, Stacy TL, Morrison KM, Mather J, Hu YH, Milewski M (2011) A temperature compensation method for CDOM fluorescence sensors in freshwater. Limnol Oceanogr Methods 9:296–301. https://doi.org/10.4319/lom.2011.9.296

Watras CJ, Morrison KA, Crawford JT, McDonald CP, Oliver SK, Hanson PC (2015) Diel cycles in the fluorescence of dissolved organic matter in dystrophic Wisconsin seepage lakes: implications for carbon turnover. Limnol Oceanogr 60:482–496. https://doi.org/10.1002/lno.10026

Watras CJ, Morrison KA, Lottig NR, Kratz TK (2016a) Comparing the diel cycles of dissolved organic matter fluorescence in a clear-water and two dark-water Wisconsin lakes: potential insights into lake metabolism. Can J Fish Aquat Sci 73:65–75. https://doi.org/10.1139/cjfas-2015-0172

Watras CJ, Morrison KA, Rubsam JL (2016b) Effect of DOC on evaporation from small Wisconsin lakes. J Hydrol 540:162–175. https://doi.org/10.1016/j.jhydrol.2016.06.002

Weyhenmeyer GA, Karlsson J (2009) Nonlinear response of dissolved organic carbon concentrations in boreal lakes to increasing temperatures. Limnol Oceanogr 54:2513–2519. https://doi.org/10.4319/lo.2009.54.6_part_2.2513

Williams CJ, Yamashita Y, Wilson HF, Jaffé R, Xenopoulos MA (2010) Unraveling the role of land use and microbial activity in shaping dissolved organic matter characteristics in stream ecosystems. Limnol Oceanogr 55:1159–1171. https://doi.org/10.4319/lo.2010.55.3.1159

Williamson CE, Overholt EP, Pilla RM, Leach TH, Brentrup JA, Knoll LB, Mette EM, Moeller RE (2015) Ecological consequences of long-term browning in lakes. Sci Rep. https://doi.org/10.1038/srep18666

Xylem (2019) EXO user manual. Yellow Spring, Ohio. https://www.ysi.com/File%20Library/Documents/Manuals/EXO-User-Manual-Web.pdf

Zhang Y, van Dijk MA, Liu M, Zhu G, Qin B (2009) The contribution of phytoplankton degradation to chromophoric dissolved organic matter (CDOM) in eutrophic shallow lakes: field and experimental evidence. Water Res 43:4685–4697. https://doi.org/10.1016/j.watres.2009.07.024

Zhang J, Hudson J, Neal R et al (2010) Long-term patterns of dissolved organic carbon in lakes across eastern Canada: evidence of a pronounced climate effect. Limnol Oceanogr 55:30–42. https://doi.org/10.4319/lo.2010.55.1.0030

Zwart JA, Sebestyen SD, Solomon CT, Jones SE (2017) The influence of hydrologic residence time on lake carbon cycling dynamics following extreme precipitation events. Ecosystems 20:1000–1014. https://doi.org/10.1007/s10021-016-0088-6